Nano Research
DOI 10.1007/s12274-014-0692-8
Research Article
ISSN 1998-0124
CN 11-5974/O4

Significant enhancement of UV emission of ZnO nanorods subject to Ga+ ion beam irradiation

Boluo Yadian[a], Rui Chen[b], Hai Liu[a], Handong Sun[b], Qing Liu[a], Chee Lip Gan[a], Zhou Kun[c], Chunwang Zhao[d], Bin Zhu[e, f, *(✉)], and Yizhong Huang[a, **(✉)]

Nano Res., **Just Accepted Manuscript** • DOI: 10.1007/s12274-014-0692-8
http://www.thenanoresearch.com on December 16 2014

Just Accepted

TSINGHUA UNIVERSITY PRESS Springer

TABLE OF CONTENTS (TOC)

Significant enhancement of UV emission of ZnO nanorods subject to Ga+ ion beam irradiation

Boluo Yadiana, Rui Chenb, Hai Liua, Handong Sunb, Qing Liua, Chee Lip Gana, Zhou Kunc, Chunwang Zhaod, Bin Zhue, f, *, and Yizhong Huanga, **

a School of Materials Science and Engineering, Nanyang Technological University, 50 Nanyang Avenue, 639798, Singapore

b Division of Physics and Applied Physics, School of Physical and Mathematical Sciences, Nanyang Technological University, 21 Nanyang Link, 637371, Singapore

c School of Mechanical and Aerospace Engineering Nanyang Technological University, 50 Nanyang Avenue, 639798, Singapore

d College of Science, Inner Mongolia University of Technology, Hohhot, 010051, China

e Department of Energy Technology, Royal Institute of Technology (Sweden)

f Hubei Collaborative Innovation Center for Advanced Materials, Faculty of Physics and Electronic Technology, Hubei University, Wuhan, Hubei 430062, P.R. China

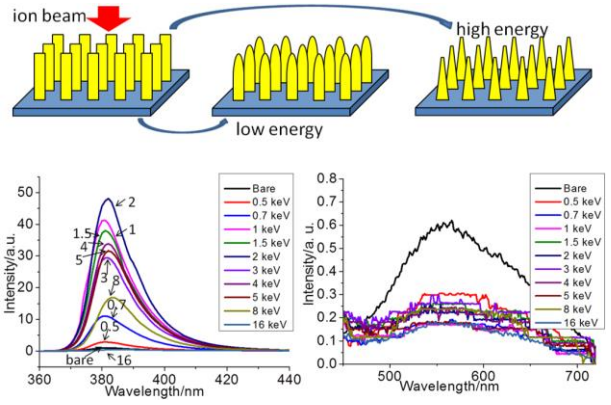

UV emission of ZnO nanorods is significantly enhanced after the irradiation of low energy Ga^{+} ion beam. We contribute this enhancement to the elimination of the surface defects and the compressive strain introduced by the ion beam.

Nano Research
DOI (automatically inserted by the publisher)
Research Article
ISSN 1998-0124
CN 11-5974/O4

Significant enhancement of UV emission of ZnO nanorods subject to Ga+ ion beam irradiation

Boluo Yadian[a], Rui Chen[b], Hai Liu[a], Handong Sun[b], Qing Liu[a], Chee Lip Gan[a], Zhou Kun[c], Chunwang Zhao[d], Bin Zhu[e, f, *(✉)], and Yizhong Huang[a, **(✉)]

a School of Materials Science and Engineering, Nanyang Technological University, 50 Nanyang Avenue, 639798, Singapore
b Division of Physics and Applied Physics, School of Physical and Mathematical Sciences, Nanyang Technological University, 21 Nanyang Link, 637371, Singapore
c School of Mechanical and Aerospace Engineering Nanyang Technological University, 50 Nanyang Avenue, 639798, Singapore
d College of Science, Inner Mongolia University of Technology, Hohhot, 010051, China
e Department of Energy Technology, Royal Institute of Technology (Sweden)
f Hubei Collaborative Innovation Center for Advanced Materials, Faculty of Physics and Electronic Technology, Hubei University, Wuhan, Hubei 430062, P.R. China

Received: day month year
Revised: day month year
Accepted: day month year (automatically inserted by the publisher)

KEYWORDS
ZnO nanrods;
photoluminescence enhancement;
UV emission;
Ga^+ ion beam

ABSTRACT

The applications of ZnO nanomaterials in optoelectronics are still limited due to their insufficient photoluminescence efficiency. In order to optimize the photoluminescence properties of ZnO nanorods, UV emission of vertically aligned ZnO nanorods grown on Si substrate in correlation with Ga^+ ion irradiation at different ion energies (0.5 keV - 16 keV) is investigated in the present paper. We found that the UV intensity increases rapidly with the increase of Ga^+ ion energy up to the maximum around 2 keV, approximately 50 times higher than the intensity produced from as-grown ZnO nanorods. The gentle bombardment of low energy Ga^+ ions removes defects from ZnO nanorod surfaces. The Ga^+ ions, on the other hand, implant into the nanorods resulting in compressive strain. It is believed that the perfect arrangement of crystal lattice upon removal of surface defects and the introduction of compressive strain are two factors that contribute the significant enhancement of UV light generation.

1 Introduction

ZnO is promising to act as building blocks for short wavelength excitonic devices due to its wide direct band gap (3.37 eV) and large exciton binding energy (60 meV) [1, 2]. In a typical photoluminescence (PL) spectrum, the room temperature emission from ZnO consists of a sharp ultraviolet (UV) emission and a wide green to red band emission (broad deep level emission, or DLE) [3]. The UV peak is the near

Address correspondence to Yizhong Huang, YZHuang@ntu.edu.sg; Bin Zhu, binzhu@kth.se

band-gap emission (NBE) of ZnO, while the DLE is attributed to the recombination of photo-generated holes with singly ionized charge states at the defects, which are usually explained by the large surface-to-volume ratio and the corresponding numerous surface states of ZnO nanomaterials [4-6]. The suppression of the DLE and the enhancement of the UV emission remain challenging for the applications of ZnO nanomaterials due to their insufficient photoluminescence efficiency. Numerous methods have been proposed to achieve this target, most of which are focused on surface passivation, such as plasma treatment [7-9], argon ion (Ar^+) milling [10, 11], introducing of surface plasmon [12, 13], or covering with dielectric layer [14-16]. However, the method that involves the facile procedure and allows the significant enhancement of UV emission has been hardly reported so far.

Lin et al. used hydrogen plasma successfully to implant ZnO nanorods to improve their PL performance [9]. The implantation depth of this method can be controlled by the bias voltage. However, they found the implantation was not stable. The PL spectra of ZnO nanorods were restored to original state after annealing process. Chen et al. used argon ion beam to mill ZnO nanorods and also found the NBE intensity was increased by a ratio of 3.25, which was ascribed to the exciton localization [11]. Since the coupling of surface plasmon resonance enables the enhancement of the PL emission, many researchers have made attempt to coat metal nanoparticles, graphene, and other hybrid nanostructures onto ZnO nanostructures [12, 13]. Dielectric materials, such as polymers and metal oxides, were also decorated on the surface of ZnO nanostructures to suppress the nonradiative process [14, 15]. Liu et al. combined these two coating methods by coating ZnO nanowires with Al_2O_3 dielectric layer through atomic layer deposition (ALD) followed by sputtering with metal nanoparticles [16]. This method is rather complicated and not reliable although they claimed the high enhancement ratio (up to several hundred).

In the present paper, the as-grown ZnO nanorods were irradiated by Ga^+ ion beam with different energies and different times in a focused ion beam (FIB) system. Then PL spectra were acquired from these ZnO nanorod samples. It was found that ZnO nanorods irradiated by Ga^+ ion beam with energy lower than 5 kV showed significantly enhanced PL performance. The UV emission could be increased by over 30 times when treated by ion beam with appropriate energy. In contrast, if the energy of the ion beam is larger than 5 kV, the UV emission reduces. The intensity of the enhancement also strongly depends on the irradiation time/dose. The UV peak rises with the increasing irradiation time of the low energy ion beam, until it reaches the highest intensity. High resolution transmission electron microscopy (HRTEM) images were collected from the ZnO nanorods before and after the ion beam milling. Before the irradiation, the ZnO nanorods were found to be covered with a shell which consists of numerous defects. This shell was removed as a result of the irradiation. Besides, compressive strain along the a-axis of the ZnO nanorods was found after the ion beam irradiation, which was also considered to the enhancement of UV emission. The subsequent decay of the UV emission of the sample irradiated by higher energy ion beam is caused by the damage and amorphorization subject to the ion beam.

2 Results and Discussion

The investigation of morphological evolution of ZnO nanorods subjected to Ga^+ ion periodical irradiation was carried out in a scanning electron microscope (SEM) with the equal ion dose (around 134 C/m^2) but different energies starting from as-grown nanorods (Fig. 1(a)). No significant changes were observed after the irradiation at energy of 2 keV, except that the nanorods are pared at the top, especially those in well alignment with the ion beam (Fig. 1(b)). The nanorods are further tapered at higher energies (Fig. 1(c) produced by ion energy of 5 keV and Fig. 1(d) by 16 keV). All nanorods are transformed into sharp nanoneedles after the ion sputtering at the energy of 30 keV (Fig. 1(f)). The process and the transformation of the morphology against low and high energies are illustrated in Fig. 1(g).

Figures 2(a) and (b) show the room temperature PL spectra of the ZnO nanorods before and after the

irradiation by Ga^+ ion beam with the same dose (134 C/m^2) but different energies, where two peaks are visible. One is NBE peak associated with the intrinsic bandgap of ZnO shown in Fig. 2(a) and the other is DLE peak generated from defects and located in the visible region as seen in Fig. 2(b). The intensity of NBE peak as a function of the energies of ion beam is plotted in Fig. 2(c). It is found that the intensity increases rapidly with the increase of Ga^+ ion energy up to the maximum at 2 keV, approximately 50 times higher than the intensity produced from as-grown nanorods, and then drops down at a slow rate. Meanwhile, the DLE peaks are also seen to be suppressed across various ion energies as shown in Fig. 2(b).

It is also interesting to mention that a slight red shift of the NBE peaks occurs after ion irradiation, as shown in Fig. 2(d), a plot of the central wavelength corresponding to the NBE peak against ion energy. The red shift of the NBE peak implies that quantum confinement effect couldn't be the reason of the enhancement, since it causes blue shift instead [17]. Several mechanisms have been proposed to explain similar red shift, such as heating effect [18], uniaxial stress/strain [19], or the contributions of excitionic emission and their phonon replicas [20]. In our experiments, the reason of the red shift is probably the ion implantation and the a-axis compressive strain introduced during the irradiation. We will discuss it in detail below.

It has become a general consensus that a lot of defects are presented near the surface of ZnO nanostructures with a large specific surface area, which gives rise to strong green DLE and low intensity of UV emission [21, 22]. Figure 3, a HRTEM image taken at a zone axis of [0 0 1], shows an area near the side wall of an as-grown ZnO nanorod. It is seen to be decorated by a thin layer of strongly distorted ZnO lattice, with the thickness of around 2.5 nm. As a result, a great number of dislocations are generated inside this layer and at the interface between this distorted lattice and the inner perfect ZnO lattice. These defects would act as the recombination centers in the ZnO nanorods and attribute to the insufficient PL efficiency [23]. However, the significant increase of UV emission occurs after the irradiation of ion beam at the energy of 3 keV. As shown in Fig. 4(a), after the gentle bombardment of Ga^+ ions, the distorted layer is removed from ZnO nanorod surfaces, which are free from defects. Therefore, the DLE is suppressed and the NBE is enhanced accordingly.

The Ga^+ ions, on the other hand, implant into the nanorods and introduce point defects in the ZnO. These point defects are probably the reason of the formation of compressive strain along a-axis, as proved by the strain mapping result in Fig. 4(b). No strain is detected along c-axis (Fig. 4(c)). This a-axis compressive strain may also be one of the reasons resulting in the UV enhancement, which is consistent with the work of Yang et al. [24]. Besides, Li et al. reported based on their calculation that the decrease of bandgap of ZnO along uniaxial a-axis compressive strain is attributed to the variation of hybridization of atomic orbits [25]. Thus this compressive strain observed after low energy irradiation is likely one of reasons that causes the red shift of the UV emission, as shown in Fig. 2(d).

Subsequently, the ZnO nanorods, subject to ion irradiation at sufficiently high energy (i.e. 16 keV), are found to produce the UV intensity as low as the as-grown nanorods (Fig. 2(c)). This is due to Ga^+ ions that sputter ZnO nanorods leading to a severe damage of their surfaces. Figure 5(a) shows a HRTEM image of the ZnO nanorods after ion irradiation with the high energy of 16 keV, where the edge appears very rough and is decorated by a thin amorphous layer. In addition, the strains along both c-axis and a-axis of the ZnO are close to zero, though slight tensile strain is shown along c-axis (Fig. 5(b)) and little compressive along a-axis (Fig. 5(c)).

The ion implantation may also contribute to the red shift of the UV peak after heavy doping. As we know in heavily doped ZnO, the bandgap is determined by two factors: (1) Burstein-Moss effect (B-M effect) which increases the bandgap [26]; (2) Urbach tail which decreases the bandgap [27]. The total bandgap could be described by the following equation [28]:

$$E_g = E_{g0} + \Delta E_g^{BM} - \Delta E_g^{W} \quad (1)$$

In which E_{g0} is the original bandgap without any

implantation, ΔE_g^{BM} and ΔE_g^{W} are the bandgap shift from B-M effect and Urbach tail, respectively. Under the condition of high concentration of the Ga^+ ions, $\Delta E_g^{BM} < \Delta E_g^{W}$. Therefore the bandgap decreases, and a red shift of the UV emission occurs. This also explains that the red shift is even larger although the a-axis compressive strain no longer exists after high energy irradiation.

Figure S1 in the Electronic Supplementary Material (ESM) shows the TEM images of the ZnO nanorod after irradiation by Ga^+ ion beam with energy as high as 30 kV and dose of 134 C/m^2. It is found that a continuous and identical amorphous layer with the thickness of around 1.2 nm is formed. This amorphous layer is probably the result of the damage introduced by the high energy ion beam. From the indexed FFT pattern inset in Fig. S1(b), we can see a new group of diffraction points, which can be identified to be $ZnGa_2O_4$ with the zone axis of [2 1 6]. Although we are not able to see the new phase of $ZnGa_2O_4$ in the TEM image of Fig. S1(b), when the doses of incident ion beam are sufficiently high, numerous particles are observed and decorated over the surface of the damaged ZnO nanorod, as shown in Fig. S1(c). The HRTEM image and the inset FFT pattern clearly prove that $ZnGa_2O_4$ nanoparticles with the diameter of around 10 nm are formed. This finding is in agreement with the literature [29], which reports that in Ga-doped ZnO system, a new phase of $ZnGa_2O_4$ will be formed when the atomic ratio of Ga is over 7 %. Thus, the observation of these $ZnGa_2O_4$ nanoparticles suggests that Ga^+ ions are implanted into ZnO nanorods under high energy irradiation. The implantation depth of is dependent of the energy of the incident ion beam.

It was found that extremely high UV emission of ZnO nanorods can be achieved by supplying Ga^+ ion dose at a constant energy below 5 keV. Figure 6(a) shows PL spectra of the ZnO nanorods irradiated by Ga^+ ion beam at 3 keV as a function of ion dose. The curve of NBE peak intensity versus the ion beam dose is plotted in Fig. 6(b). It is clear that the intensity of the NBE peak increases around 30 times more when the dose is high enough. The enhancement seems to be saturated when the dose is increased to over 268 C/m^2, as the PL spectra of 268 C/m^2 and 402 C/m^2 are almost the same, which can be seen clearly in the inset of Fig. 6(a). The same ion irradiation procedure with irradiation energies of 1 keV and 5 keV is repeated with the results presented in Fig. S2 in the ESM, and similar phenomena are observed.

3 Conclusions

We present a strategy for tailoring the optical properties of ZnO nanorods through the study of the photoluminescence and morphology of the ZnO nanrods irradiated by the Ga^+ ion beam. It is found that the intensity of the band edge luminescence strongly depends on the ion beam energy and dose. As a result of the Ga^+ ion beam irradiation with the energy in the range of 1~5 kV and the dose of 134 C/m^2, NBEs can be enhanced by over 30 times, while the DLEs are suppressed. We contribute this enhancement to the elimination of the surface defects and the compressive strain introduced by the ion beam. This dramatic enhancement of the NBEs and the suppression of DLEs through Ga^+ ion beam irradiation may have potential applications in photovoltaic devices.

4 Experimental Section

4.1 Growth of ZnO nanorods

ZnO seed layer with the thickness of around 50 nm was deposited onto the surface of Si wafer evenly through a radio frequency (RF) magnetron sputtering system (Kurt. J. Lesker, USA). The ZnO/Si substrate was subsequently immersed into the mixed solution of Zinc Nitrate Hexahydrate ($Zn(NO_3)_2{\cdot}6H_2O$) (≥98%, Sigma-Aldrich, USA) and Hexamethylenetetramine (HMTA) (≥99.5%, Sigma-Aldrich, USA) facing downward, and then heated at the temperature of 90℃ for three hours. Finally the sample was retrieved, rinsed in DI water and dried in air at room temperature.

4.2 Irradiation with Ga^+ ion beam

ZnO/Si substrate with ZnO nanorods were subjected to the Ga^+ ion beam in the FIB system perpendicular to the substrates. For comparison, Ga^+ ion irradiation was carried out on the surfaces of two samples with one sample that was irradiated to a sequence of

square patterns (20 μm × 20 μm) using different ion voltages and the other where a series of identical squares was ion beam scanned with different scanning times. The ion irradiation fluence rates under different voltages are listed in Table S1 in the ESM.

4.3 Characterization

SEM images were collected in the dual beam FIB system (Nova Nanolab 600i, FEI, USA). TEM images were captured on 2100F (JEOL, Japan) at the electron beam energy of 200 keV to analyze the microstructure of ZnO nanorods before and after Ga^+ ion beam treatment.

4.4 PL Measurement

PL measurements were performed at room temperature with a home-made micro-PL system, using a He-Cd laser (laser line 325 nm) as excitation source. A 750 mm monochromator with suitable filters was used to disperse the signal, which was then detected by a photomultiplier through standard lock-in amplifier technique.

Acknowledgements

This research was support by SUG (Start-up funding in NTU), Tier 1 (AcRF grant MOE Singapore M401992), Tier 2 (AcRF grant MOE Singapore M4020159) and the Chinese Natural Science Foundation (Grant 60906053, 62174118 and 51308050309).

Electronic Supplementary Material: Supplementary material is available in the online version of this article at http://dx.doi.org/10.1007/s12274-***-****-*, including the following contents: (a) ion irradiation fluence rates under different voltages used in the experiements; (b) TEM images of the ZnO nanorods irradiated by ion beam with extremely high voltages or large dose; (c) PL performance after the treatment of ion beam (1 kV or 5 kv) with varying dose for comparison.

References

[1] Tang, Z. K.; Wong, G. K. L.; Yu, P.; Kawasaki, M.; Ohtomo, A.; Koinuma, H.; Segawa, Y. Room-temperature ultraviolet laser emission from self-assembled ZnO microcrystallite thin films. *Appl. Phys. Lett.* **1998**, *72*, 3270-3272.

[2] Zhang, B. P.; Binh, N. T.; Wakatsuki, K.; Segawa, Y.; Yamada, Y.; Usami, N.; Kawasaki, M.; Koinuma, H. Formation of highly-aligned ZnO tubes on sapphire (0001) substrates. *Appl. Phys. Lett.* **2004**, *84*, 4098-4100.

[3] Zeng, H.; Duan, G.; Li, Y.; Yang, S.; Xu, X.; Cai, W. Blue Luminescence of ZnO Nanoparticles Based on Non-Equilibrium Processes: Defect Origins and Emission Controls. *Adv. Funct. Mater.* **2010**, *20*, 561-572.

[4] Ozgur, U.; Alivov, Y. I.; Liu, C.; Teke, A.; Reshchikov, M. A.; Dogan, S.; Avrutin, V.; Cho, S. J.; Morkoc, H. A comprehensive review of ZnO materials and devices. *J. Appl. Phys.* **2005**, *98*, 041301.

[5] Kim, T. W.; Kazawoe, T.; Yamazaki, S.; Ohtsu, M.; Sekiguchi, T. Low-temperature orientation-selective growth and ultraviolet emission of single-crystal ZnO nanowires. *Appl. Phys. Lett.* **2004**, *84*, 3358-3360.

[6] Yadian, B.; Liu, H.; Wei, Y.; Wu, J.; Zhang, S.; Sun, L.; Zhao, C.; Liu, Q.; Ramanujan, R. V.; Zhou, K.; Gan, C. L.; Huang, Y. Towards Perfectly Ordered Novel ZnO/Si Nano-heterojunction Arrays. *Small* **2013**, *10*, 344-348.

[7] Yang, Y.; Tay, B. K.; Sun, X. W.; Sze, J. Y.; Han, Z. J.; Wang, J. X.; Zhang, X. H.; Li, Y. B.; Zhang, S. Quenching of surface-exciton emission from ZnO nanocombs by plasma immersion ion implantation. *Appl. Phys. Lett.* **2007**, *91*, 071921.

[8] Yang, Y.; Sun, X. W.; Tay, B. K.; Cao, P. H.; Wang, J. X.; Zhang, X. H. J. Revealing the surface origin of green band emission from ZnOnanostructures by plasma immersion ion implantation induced quenching. *Appl. Phys.* **2008**, *103*, 064307.

[9] Lin, C. C.; Chen, H. P.; Liao, H. C.; Chen, S. Y. Enhanced luminescent and electrical properties of hydrogen-plasma ZnO nanorods grown on wafer-scale flexible substrates. *Appl. Phys. Lett.* **2005**, *86*, 183103.

[10] Chen, R.; Ye, Q. L.; He, T. C.; Wu, T.; Sun, H. D. Uniaxial tensile strain and exciton–phonon coupling in bent ZnO nanowires. *Appl. Phys. Lett.* **2011**, *98*, 241916.

[11] Chen, R.; Ye, Q. L.; He, T.; Ta, V. D.; Ying, Y.; Tay, Y. Y.; Wu, T.; Sun, H. Exciton Localization and Optical Properties Improvement in Nanocrystal-Embedded ZnO Core–Shell Nanowires. *Nano Lett.* **2013**, *13*, 734-739.

[12] Hwang, S. W.; Shin, D. H.; Kim, C. O.; Hong, S. H.; Kim, M. C.; Kim, J.; Lim, K. Y.; Kim, S.; Choi, S. H.; Ahn, K. J.; Kim, G.; Sim, S. H.; Hong, B. H. Plasmon-Enhanced Ultraviolet Photoluminescence from Hybrid Structures of Graphene/ZnO Films. *Phys. Rev. Lett.* **2010**, *105*, 127403.

[13] Shao, D.; Sun, H.; Yu, M.; Lian, J.; Sawyer, S. Enhanced ultraviolet emission from poly(vinyl alcohol) ZnO nanoparticles using a SiO2-Au core/shell structure. *Nano Lett.* **2012**, *12*, 5840-5844.

[14] Richters, J. P.; Voss, T.; Wischmeier, L.; Ruckmann, I.; Gutowski, J. Influence of polymer coating on the low-temperature photoluminescence properties of ZnO nanowires. *Appl. Phys. Lett.* **2008**, *92*, 011103.

[15] Liu, K. W.; Chen, R.; Xing, G. Z.; Wu, T.; Sun, H. D. Photoluminescence characteristics of high quality ZnO nanowiresand its enhancement by polymer covering. *Appl. Phys. Lett.* **2010**, *96*, 023111.

[16] Liu, M.; Chen, R.; Adamo, G.; MacDonald, K. F.; Sie, E. J.; Sum, T. C.; Zheludev, N. I.; Sun, H.; Fan, H. J. Tuning the

influence of metal nanoparticles on ZnO photoluminescence by atomic-layer-deposited dielectric spacer. *Nanophotonics* **2013**, *2*, 153-160.

[17] Lin, K. F.; Cheng, H. M.; Hsu, H. C.; Lin, L. J.; Hsieh, W. F. Band gap variation of size-controlled ZnO quantum dots synthesized by sol–gel method. *Chem. Phys. Lett.* **2005**, *409*, 208-211.

[18] Yang, Y.; Yan, H.; Fu, Z.; Yang, B.; Xia, L.; Xu, Y.; Zuo, J.; Li, F. Photoluminescence Investigation Based on Laser Heating Effect in ZnO-Ordered Nanostructures. *J. Phys. Chem. B* **2005**, *110*, 846-852.

[19] Yan, B.; Chen, R.; Zhou, W. W.; Zhang, J. X.; Sun, H. D.; Gong, H.; Yu, T. Localized suppression of longitudinal-optical-phonon–exciton coupling in bent ZnO nanowires. *Nanotechnology* **2010**, *21*, 445706.

[20] Voss, T.; Bekeny, C.; Wischmeier, L.; Gafsi, H.; Borner, S.; Schade, W.; Mofor, A. C.; Bakin, A.; Waag, A. Influence of exciton-phonon coupling on the energy position of the near-band-edge photoluminescence of ZnO nanowires. *Appl. Phys. Lett.* **2006**, *89*, 182107.

[21] Yang, Y.; Sun, X. W.; Tay, B. K.; Cao, P. H. T.; Wang, J. X.; Zhang, X. H. Revealing the surface origin of green band emission from ZnO nanostructures by plasma immersion ion implantation induced quenching. *J. Appl. Phys.* **2008**, *103*, 064307.

[22] Rosenberg, R. A.; Haija, M. A.; Vijayalakshmi, K.; Zhou, J.; Xu, S.; Wang, Z. L. Depth resolved luminescence from oriented ZnO nanowires. *Appl. Phys. Lett.* **2009**, *95*, 243101.

[23] Shalish, I.; Temkin, H.; Narayanamurti, V. Size-dependent surface luminescence in ZnO nanowires. *Phys. Rev. B* **2004**, *69*, 245401.

[24] Yang, Q.; Wang, W.; Xu, S.; Wang, Z. L. Enhancing Light Emission of ZnO Microwire-Based Diodes by Piezo-Phototronic Effect. *Nano Lett.* **2011**, *11*, 4012-4017.

[25] Shi, L. B.; Cheng, S.; Li, R. B.; Kang, L.; Jin, J. W.; Li, M. B. A study on strain affecting electronic structure of Wurtzite ZnO by first principles. *Mod. Phys. Lett. B* **2009**, *23*, 2339-2352.

[26] Bhosle, V.; Tiwari, A.; Narayan, J. Metallic conductivity and metal-semiconductor transition in Ga-doped ZnO. *Appl. Phys. Lett.* **2006**, *88*, 032106.

[27] Ilican, S.; Caglar, Y.; Caglar, M.; Yakuphanoglu, F. Structural, optical and electrical properties of F-doped ZnO nanorod semiconductor thin films deposited by sol-gel process. *Appl. Surf. Sci.* **255**, *2008*, 2353-2359.

[28] Hou, Q.; Zhao, C.; Jin, Y.; Guan, Y.; Lin, L.; Li, J. Effects of the concentration of Ga high doping on electric conductivity and red shift of ZnO from frist principles. *Acta Phys. Sin.* **2010**, *59*, 4156-4161.

[29] Zhou, K. Fabrication of Ga-doped transparent ZnO film and investigation of its photoelectronic properties. MD. Dissertation, College of Physics of Chongqing University, Chongqing, China, 2010, 39-44.

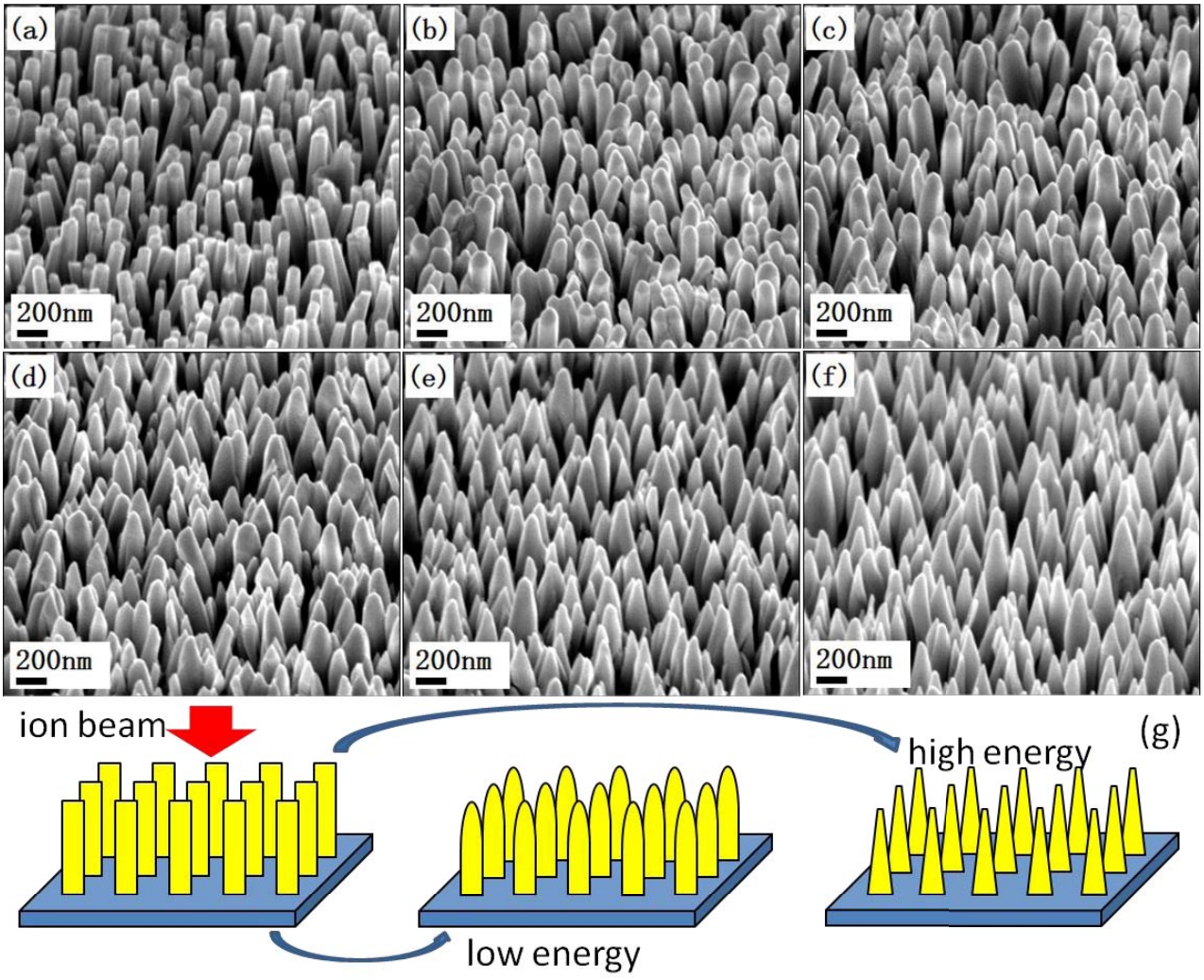

Figure 1 SEM images of ZnO nanorods irradiated by Ga ion beam with different energies: (a) without ion beam irradiation; (b) 2 keV; (c) 5 keV; (d) 8 keV; (e) 16 keV; (f) 30 keV; (g) schematic illustration of the ion irradiation process under low and high engergies

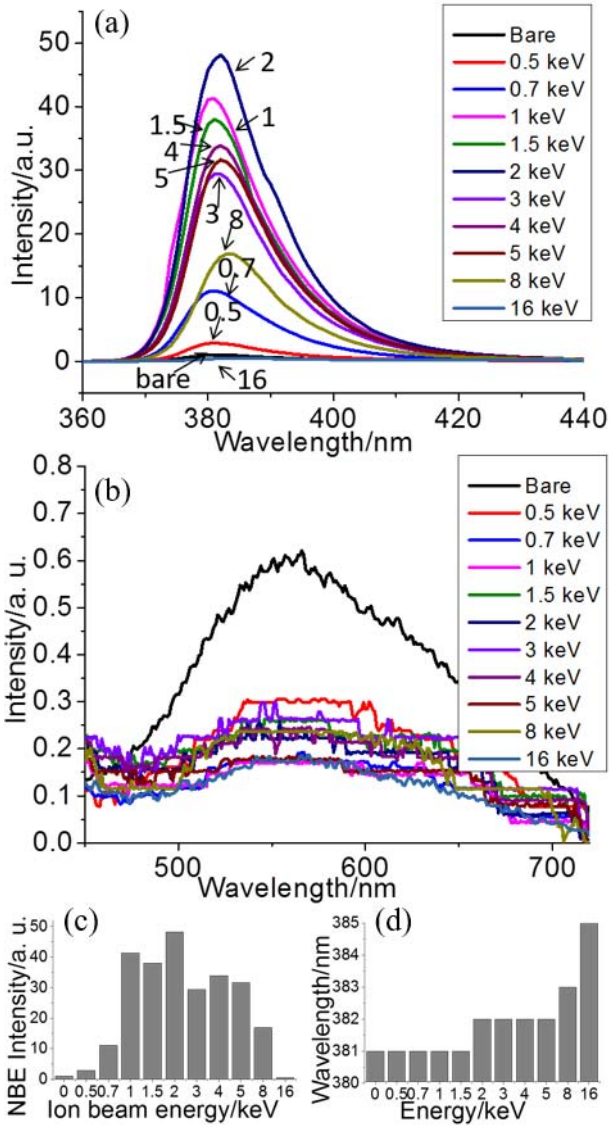

Figure 2 (a) UV emission of ZnO nanorods irradiated by Ga^+ ion beam (the numbers and arrows indicate the energies of the ion beam used); (b) emission of ZnO nanorods in the visible range; (c) Intensity of the NBE peaks of the ZnO nanorods after the irradiation; (d) the position of the NBE peaks after the irradiation.

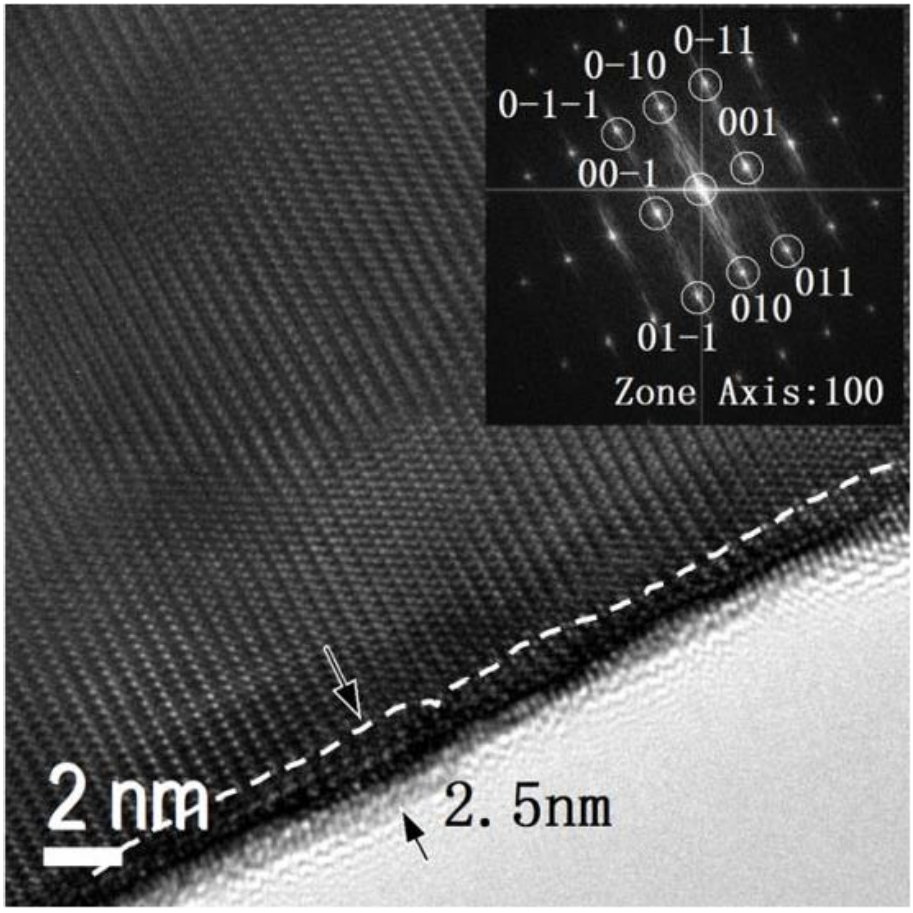

Figure 3 HRTEM image of the edge of the ZnO nanorod without ion beam irradiation and the corresponding FFT pattern

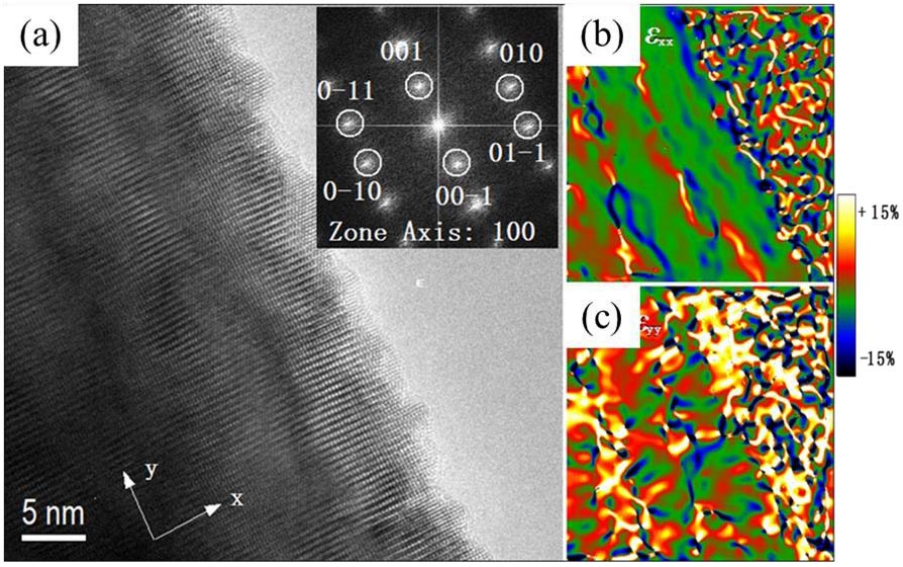

Figure 4 (a) HRTEM image of the edge of the ZnO nanorod irradiated by 3 keV Ga^+ ion beam; (b) the strain mapping result along the a-axis; (c) the strain mapping result along the c-axis. (Positive value indicates tensile strain; negative value indicates compressive strain)

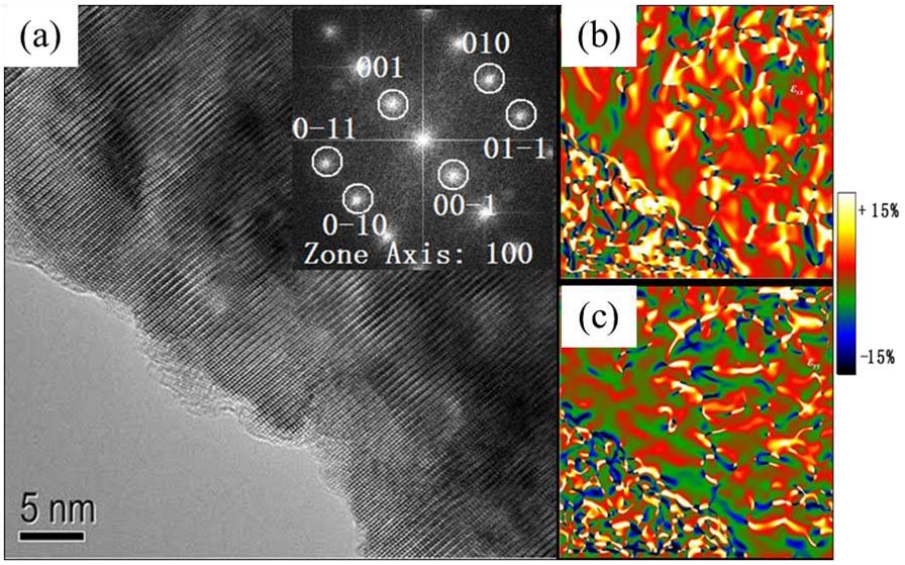

Figure 5 (a) HRTEM image of the edge of the ZnO nanorods irradiated by 16 kV Ga^+ ion beam; (b) the strain mapping result along the a-axis; (c) the strain mapping result along the c-axis.

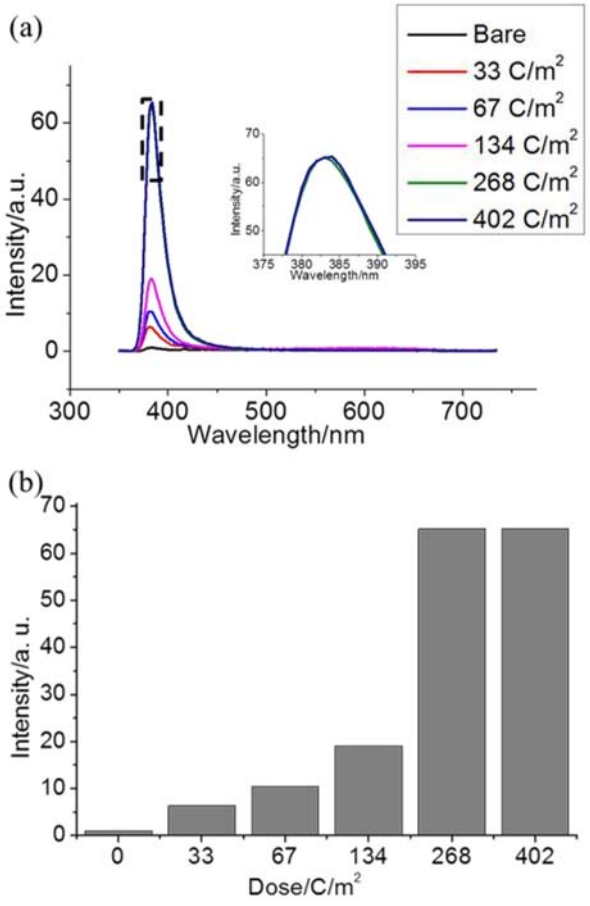

Figure 6 (a) PL results of ZnO nanorods irradiated by 3 keV Ga ion beam with different times; (b) the intensity of the NBE peaks of ZnO nanorods irradiated by 3 keV Ga^+ ion beam with different times.

Electronic Supplementary Material

Significant enhancement of UV emission of ZnO nanorods subject to Ga+ ion beam irradiation

Boluo Yadian[a], Rui Chen[b], Hai Liu[a], Handong Sun[b], Qing Liu[a], Chee Lip Gan[a], Zhou Kun[c], Chunwang Zhao[d], Bin Zhu[e, f, *(✉)], and Yizhong Huang[a, **(✉)]

a School of Materials Science and Engineering, Nanyang Technological University, 50 Nanyang Avenue, 639798, Singapore
b Division of Physics and Applied Physics, School of Physical and Mathematical Sciences, Nanyang Technological University, 21 Nanyang Link, 637371, Singapore
c School of Mechanical and Aerospace Engineering Nanyang Technological University, 50 Nanyang Avenue, 639798, Singapore
d College of Science, Inner Mongolia University of Technology, Hohhot, 010051, China
e Department of Energy Technology, Royal Institute of Technology (Sweden)
f Hubei Collaborative Innovation Center for Advanced Materials, Faculty of Physics and Electronic Technology, Hubei University, Wuhan, Hubei 430062, P.R. China

Supporting information to DOI 10.1007/s12274-****-****-* (automatically inserted by the publisher)

Address correspondence to Yizhong Huang, YZHuang@ntu.edu.sg; Bin Zhu, binzhu@kth.se

Ga^+ ion irradiation fluence

The irradiation fluence rate is proportional to the ion beam current density. In the FIB system, the beam current density is changed according to the alignment setting when the ion beam energy (the applied voltage) changes. Calculated irradiation fluencies of the ion beam in detail are listed in the following Table S1:

Table S1 Irradiation fluencies at different voltages used in the article.

Voltage/kV	Current/pA	Scanned Area/μm^2	Current Density/pA/μm^2	Irradiation Fluence/$10^6/\mu m^2/s$
0.5	110	400	0.275	1.72
0.7	80	400	0.2	1.25
1	36	400	0.09	0.56
1.5	27	400	0.0675	0.42
2	28	400	0.07	0.44
3	34	400	0.085	0.53
4	40	400	0.1	0.63
5	47	400	0.1175	0.73
8	62	400	0.155	0.97
16	130	400	0.325	2.03
30	280	400	0.7	4.38

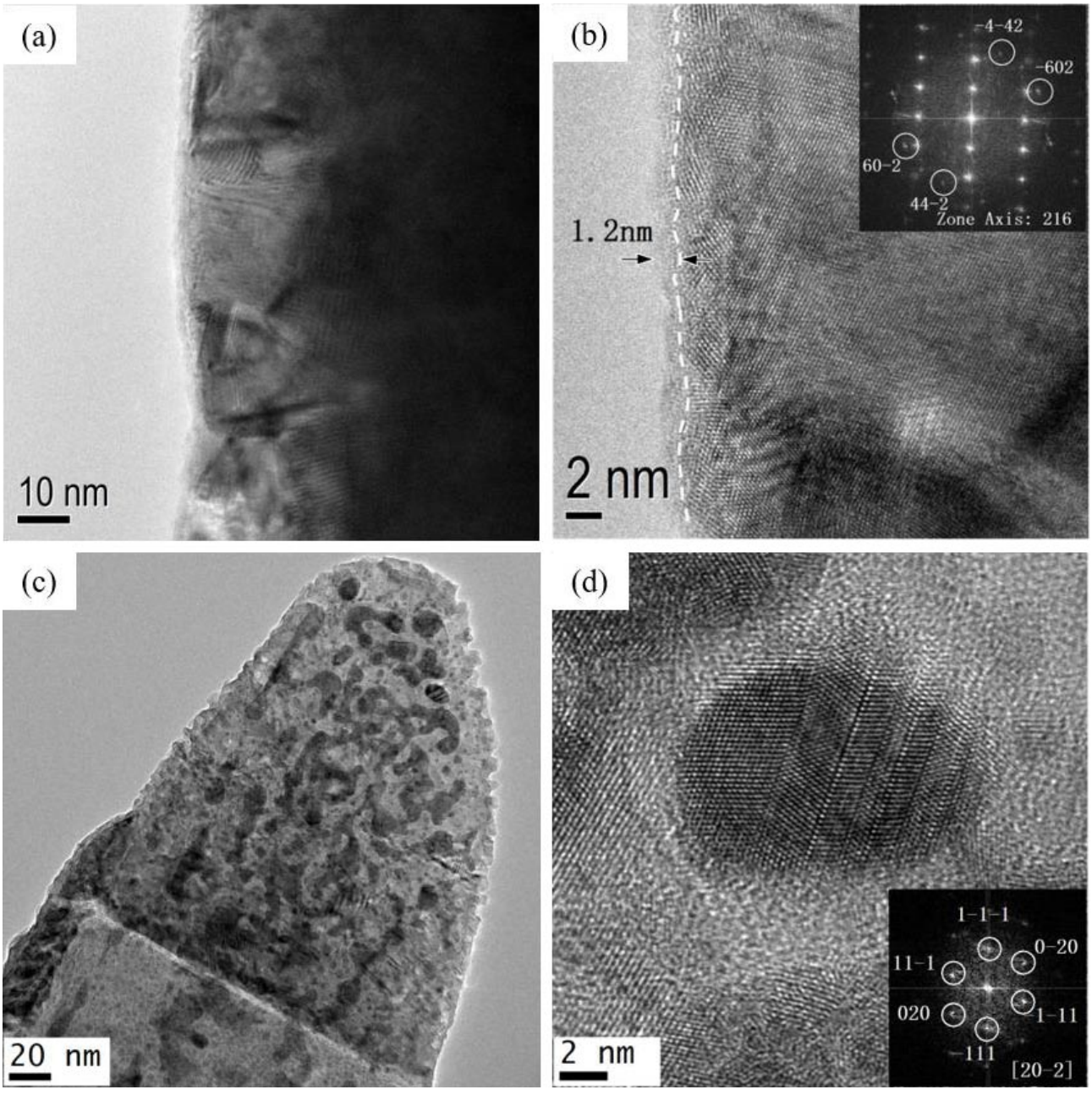

Figure S1 (a) TEM image of the edge of the ZnO nanorod irradiated by 30 kV Ga ion beam; (b) TEM image under high magnification and the corresponding FFT pattern; (c) TEM image of the ZnO nanrod after irradiation of Ga^+ ion beam with energy of 30 kV and extremely large dose; (d) HRTEM image of the circled particle in Fig. S1(c).

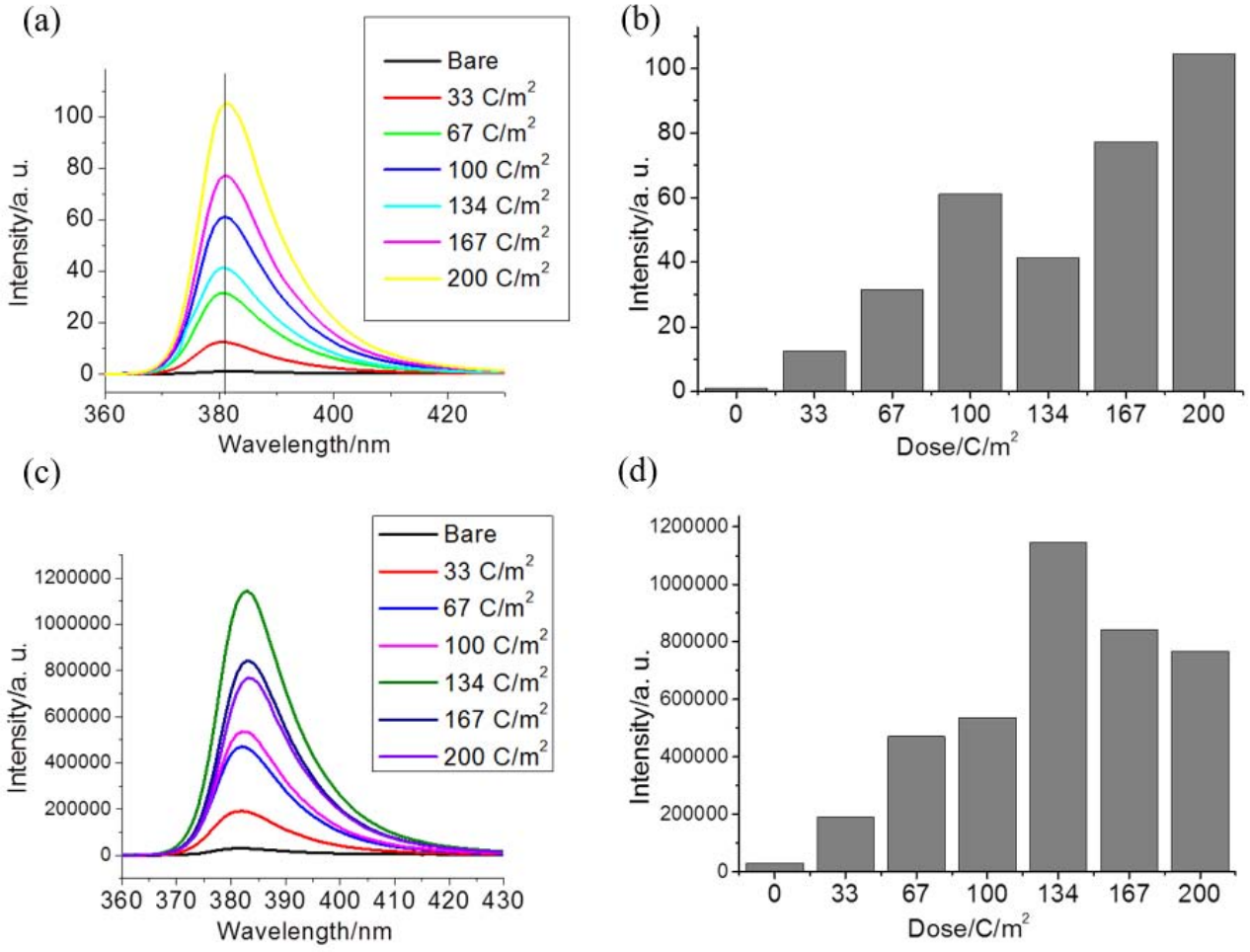

Figure S2 (a) PL results of ZnO nanorods irradiated by 1 keV Ga^+ ion beam with different doses; (b) the intensity of the UV peaks of ZnO nanorods irradiated by 1 keV ion beam with different doses; (c) PL results of ZnO nanorods irradiated by 5 keV ion beam with different doses; (d) the intensity of the UV peaks of ZnO nanorods irradiated by 5 keV ion beam with different doses.